Effect of the substituent nature on the efficiency of isoquinolines

A.G. Berezhnaya,* A.D. Zagrebaev, V.V. Chernyavina, I.I. Krotkii and V.V. Chernyavskaya

Southern Federal University, ul. Zorge 7, 344090 Rostov-on-Don, Russian Federation
**E-mail: Berezhnaya-Aleksandra@Mail.Ru*

Abstract

The protective effect of seven new isoquinoline derivatives as inhibitors of acid corrosion of low-carbon steel in 1 M hydrochloric acid has been studied. At a temperature of 298 K and a concentration of 0.1 mmol/L, the protective effect of the compounds was found to be 93–98.8% depending on the nature of the substituent. When the temperature increases to 353 K, the efficiency decreases to 80–93%. The compounds studied change the effective activation energy of corrosion, affect the structure of the double electric layer, and block a fraction of the steel surface upon adsorption. The compounds reduce the rates of cathodic and anodic processes. A satisfactory correlation of efficiency with the calculated parameters of molecules obtained within the scope of the density functional theory (DFT) B3LYP/6-311+G(d) has been found. It has been shown that the correlation coefficients of the linear relationships "protective effect – calculated characteristics" decrease with an increase in temperature.

Received: April 2, 2024 Published: May 22, 2024 doi: 10.17675/2305-6894-2024-13-2-17

Keywords: *inhibitor, acid corrosion, isoquinoline derivatives, steel.*

Introduction

Nitrogen and oxygen-containing organic compounds are often studied as inhibitors of acid corrosion of steels. Depending on their structure, they can exhibit high protective properties [1–8]. Such compounds include isoquinoline derivatives [9, 10]. The effect of the substituent at position 4 of the phenyl ring in 1-(4-**X**-phenyl)-2-(9,10-dimethoxy-13-(7-nitrobenzo[*c*][1,2,5]oxadiazol-4-yl)-5,8-dihydro-6*H*-[1,3]dioxolo[4,5-*g*]isoquinolino[3,2-*a*]isoquinolin-8-yl)ethan-1-one, where **X** = NH_2, OCH_3, or Cl, on their efficiency against steel corrosion in hydrochloric acid was studied previously [10]. A high protective effect of the compounds was found. The efficiency of the compounds was 98 and 92% at temperatures of 298 and 353 K, respectively. The protective effect of the compounds correlated well with many calculated parameters of molecules obtained in the scope of the density functional theory (DFT). Apparently, this is due to the fact that the substituents occupied the same position. The location of the functional group affects the protective effect of compounds [11], and their calculated parameters also change.

To continue studying the effect of the substituent on the inhibitory properties of isoquinolines, its new derivatives were synthesized, a quantum chemical calculation of the parameters was carried out, and their efficiency was compared with the calculation results.

Experiment

New isoquinoline derivatives with the following general formula and a variable substituent *R* have been studied:

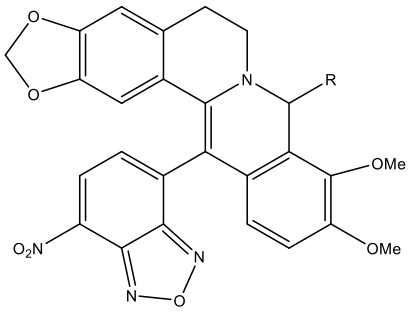

1, R= 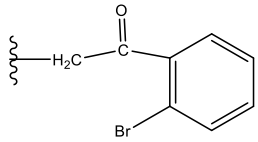

2, R= 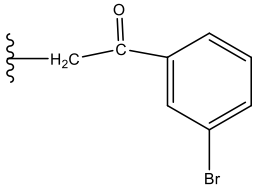

3, R= 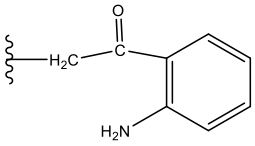

4, R= 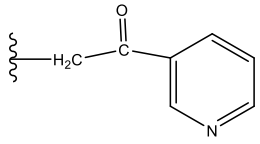

5, R= 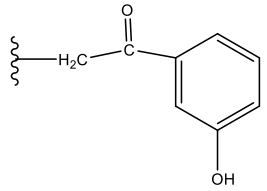

6, R= 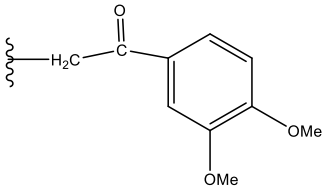

7, R= 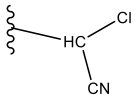

General Procedure for the Synthesis of Compounds

Reduced berberine derivatives were obtained using the known procedure [12, 13]. A sample of NaOH (2 g) was dissolved in 60 ml of 70% isopropanol solution, after which a sample of berberine of (371.81 mg, 1 mmol) was added. The solution was stirred for 20 min and then 1 mol-equiv. of the appropriate nucleophile was added with intense

stirring. After stirring the solution for 30 min, 600 ml of distilled water was added to it to precipitate the product. Next, the mixture was filtered on a Buchner funnel, and the precipitate was dried and crystallized from anhydrous methanol.

Di-substituted products were synthesized according to reported methods [12–16]. A sample of an activated berberine derivative was dissolved in DMF with stirring. One drop of triethylamine was added to the solution to stabilize the product during isolation. Next, a solution of 4-chloro-7-nitrobenzo[*c*][1,2,5]oxadiazole was prepared separately. Its equivalent sample was dissolved in DMF and cooled to 5°C. The solutions were then placed into microfluidic syringes and mixed at a rate of 2 μL/sec. The resulting mixture was kept in a dark place for an hour, after which the product was precipitated with distilled water.

^{1}H and ^{13}C NMR spectra were recorded on a Bruker DPX-250 spectrometer operating at 250 MHz and 63 MHz, respectively, using $CDCl_3$ as the solvent and TMS (tetramethylsilane) as the internal standard. Signal assignments in the ^{1}H NMR spectra were made based on the data obtained from two-dimensional COSY spectra with mixing times of 0.6–1.3 seconds. The ^{13}C NMR spectra exhibit signal overlap resulting in fewer distinct signals compared to the theoretical number of signals.

High-resolution mass spectra were recorded on a Bruker micrOTOF II instrument using electrospray ionization in positive ion mode with a capillary voltage of 4500 V. The mass scanning range was from 50 to 3000 Da. Melting points were determined using glass capillaries on a melting point apparatus (PTP).

1-(2-Bromophenyl)-2-(9,10-dimethoxy-13-(7-nitrobenzo[*c*][1,2,5]oxadiazol-4-yl)-5,8-dihydro-6*H*-[1,3]dioxolo[4,5-*g*]isoquinolino[3,2-*a*]isoquinolin-8-yl)ethan-1-one (1).
Yield 564 mg (81%), dark-green needle-shaped crystals, decomp. 119–120°C. ^{1}H NMR spectrum ($CDCl_3$), δ (*J*, Hz): 2.71–2.80 (1H, dt, *J* = 14.74, 3.62, 5-CH_2); 2.89–3.01 (1H, dt, *J* = 15.84, 7.85, 6-CH_2); 3.10–3.17 (1H, dd, *J* = 14.67, 4.12, $CH_2C(O)$); 3.47–3.52 (2H, m, 5,6-CH_2); 3.61–3.70 (1H, dd, *J* = 14.62, 7.52, $CH_2C(O)$); 3.83 (3H, s, 10-OCH_3); 3.97 (3H, s, 9-OCH_3); 5.61–5.66 (1H, dd, *J* = 7.44, 4.02, H-8); 5.78–5.79 (2H, d, *J* = 2.69, OCH_2O); 6.02 (1H, s, H-1); 6.35–6.39 (1H, d, *J* = 8.67, H-11); 6.59 (1H, s, H-4); 6.67–6.70 (1H, d, *J* = 8.76, H-12); 7.21–7.27 (2H, m, H-4′, Ar); 7.60–7.64 (1H, m, Ar); 7.78–7.81 (1H, d, *J* = 7.75, Ar); 7.96 (1H, s, Ar); 8.45–8.49 (1H, d, *J* = 7.75, H-5′). ^{13}C NMR spectrum ($CDCl_3$), δ: 30.75; 41.95; 49.38; 55.74; 56.07; 60.93; 101.23; 103.64; 107.97; 108.36; 112.05; 117.72; 122.94; 124.13; 124.81; 126.98; 127.00; 129.63; 130.12; 131.24; 131.52; 132.46; 133.41; 135.94; 138.66; 139.69; 142.29; 143.31; 143.39; 145.47; 148.01; 150.77; 151.59; 197.08. Found, *m/z*: 719.0755 $[M+Na]^+$. $C_{34}H_{25}BrN_4NaO_8^+$. Calculated, *m/z*: 719.0753.

1-(3-Bromophenyl)-2-(9,10-dimethoxy-13-(7-nitrobenzo[*c*][1,2,5]oxadiazol-4-yl)-5,8-dihydro-6*H*-[1,3]dioxolo[4,5-*g*]isoquinolino[3,2-a]isoquinolin-8-yl)ethan-1-one (2).
Yield 480 mg (69%), dark-green needle-shaped crystals, decomp. 125–126°C. ^{1}H NMR spectrum ($CDCl_3$), δ (*J*, Hz): 2.84–2.93 (2H, m, H-5); 3.60–3.67 (2H, dt, *J* = 9.33, 4.38,

H-5); 3.81 (3H, s, 10-OCH_3); 3.88–3.93 (2H, m, $CH_2C(O)$); 3.95 (3H, s, 9-OCH_3); 5.72–5.77 (1H, d, *J* = 6.56, H-8); 5.78 (2H, c, OCH_2O); 6.15 (1H, s, H-1); 6.45–6.49 (1H, d, *J* = 8.66, H-11); 6.60 (1H, s, H-4); 6.67–6.70 (1H, d, *J* = 8.71, H-12); 7.20–7.22 (1H, m, Ar); 7.27–7.30 (1H, d, *J* = 8.80, Ar); 7.35–7.39 (1H, d, *J* = 7.87, H-4′); 7.48–7.51 (1H, *J* = 8.88, Ar); 8.41–8.45(1H, *J* = 7.86, H-5′). ^{13}C NMR spectrum ($CDCl_3$), δ: 30.69; 46.31; 49.88; 54.03; 56.04; 60.99; 101.29; 103.85; 108.09; 108.60; 111.79; 117.90; 118.88; 124.81; 127.13; 127.44; 128.82; 131.50; 131.89; 132.86; 133.80; 139.52; 140.72; 143.21; 143.55; 144.21; 145.56; 148.30; 150.79; 151.41; 201.77. Found, *m/z*: 719.0754 $[M+Na]^+$. $C_{34}H_{25}BrN_4NaO_8^+$. Calculated, *m/z*: 719.0753.

1-(2-Aminophenyl)-2-(9,10-dimethoxy-13-(7-nitrobenzo[*c*][1,2,5]oxadiazol-4-yl)-5,8-dihydro-6*H*-[1,3]dioxolo[4,5-g]isoquinolino[3,2-*a*]isoquinolin-8-yl)ethan-1-one (3).
Yield 490 mg (78%), dark-green bluish needle-shaped crystals, decomp. 121–124°C. ^{1}H NMR spectrum ($CDCl_3$), δ (*J*, Hz): 2.87–2.98 (1H, m, 5-CH_2); 3.04–3.12 (1H, m, 6-CH_2); 3.44–3.59 (3H, m, 5-CH_2, $CH_2C(O)$); 3.64–3.73 (1H, m, 6-CH_2); 3.85 (3H, s, 10-OCH_3); 3.98 (3H, s, 9-OCH_3); 5.62–5.67 (1H, dd, *J* = 7.67, 3.72, H-8); 5.76–5.79 (2H, m, OCH_2O); 6.16 (1H, s, H-1); 6.41–6.43 (1H, d, *J* = 8.70, H-11); 6.47–6.63 (3H, m, H-4, Ar); 6.68–6.72 (1H, d, *J* = 8.62, H-12); 7.18–7.26 (2H, m, H-4′, Ar); 7.58–7.62 (1H, m, Ar); 8.44–8.47 (1H, d, *J* = 7.78, H-5′). ^{13}C NMR spectrum ($CDCl_3$), δ: 30.72; 42.89; 49.29; 56.09; 60.89; 101.17; 103.77; 107.90; 108.68; 111.90; 115.80; 117.03; 117.75; 118.24; 120.35; 124.80; 125.04; 127.28; 128.37; 129.07; 131.26; 131.83; 132.57; 134.50; 139.86; 143.40; 145.44; 148.00; 150.56; 150.75; 151.49; 200.33 Found, *m/z*: 669.1709 $[M+Na]^+$. $C_{34}H_{26}N_6NaO_8^+$. Calculated, *m/z*: 669.1710.

2-(9,10-Dimethoxy-13-(7-nitrobenzo[*c*][1,2,5]oxadiazol-4-yl)-5,8-dihydro-6*H*-[1,3]dioxolo[4,5-*g*]isoquinolino[3,2-*a*]isoquinolin-8-yl)-1-(pyridin-3-yl)ethan-1-one (4).
Yield 365 mg (59%), dark-green needle-shaped crystals, decomp. 98–101°C. (DMSO-d_6), δ (*J*, Hz): 2.52–2.60 (1H, m, 5-CH_2); 3.10–3.19 (1H, dd, *J* = 15.02, 7.57, 6-CH_2); 3.38–3.62 (2H, m, 5-CH_2, 6-CH_2); 3.80 (3H, s, 10-OCH_3); 3.82–3.83 (2H, m, $CH_2C(O)$); 3.88 (3H, s, 9-OCH_3); 5.42–5.47 (1H, dd, *J* = 7.62, 4.46, H-8); 5.76–5.78 (2H, dd, *J* = 5.84, 1.05, OCH_2O); 5.96–6.00 (1H, d, *J* = 10.75, H-11); 6.32 (1H, s, H-1); 6.50–6.54 (1H, d, *J* = 8.42, *o*-Ar); 6.72–6.86 (3H, m, m-Ar, H-4, H-12); 7.30–7.45 (3H, m, p-Ar, o′-Ar, H-4′); 8.44–8.47 (1H, d, *J* = 7.92, H-5′). ^{13}C NMR spectrum (DMSO-d_6), δ: 29.90; 30.07; 46.17; 49.00; 54.60; 60.26; 100.82; 101.60; 104.49; 107.70; 108.53; 108.65; 111.87; 118.37; 118.97; 124.80; 124.96; 127.18; 128.34; 128.93; 130.37; 132.19; 133.18; 138.49; 143.19; 144.07; 145.64; 148.32; 150.76; 151.49; 151.93; 206.67. Found, *m/z*: 642.1604 $[M+Na]^+$. $C_{33}H_{25}N_5NaO_8^+$. Calculated, *m/z*: 642.1601.

2-(9,10-Dimethoxy-13-(7-nitrobenzo[*c*][1,2,5]oxadiazol-4-yl)-5,8-dihydro-6*H*-[1,3]-dioxolo[4,5-*g*]isoquinolino[3,2-*a*]isoquinolin-8-yl)-1-(3-hydroxyphenyl)ethan-1-one (5).
Yield 560 mg (89%), dark-green needle-shaped crystals, decomp. 103–105°C. ^{1}H NMR spectrum ($CDCl_3$), δ (*J*, Hz): 2.71–2.80 (1H, dt, *J* = 14.51, 3.51, 5-CH_2); 2.88–2.94 (1H,

dd, J = 10.57, 5.27, 6-CH_2); 3.04–3.12 (1H, dd, J = 14.48, 3.67, $CH_2C(O)$); 3.42–3.54 (2H, td, J = 11.01, 5.20, 5-CH_2, 6-CH_2); 3.64–3.72 (1H, dd, J = 14.47, 7.75, $CH_2C(O)$); 3.85 (3H, s, 10-OCH_3); 3.98 (3H, s, 9-OCH_3); 5.62–5.67 (1H, dd, J = 7.69, 3.73, H-8); 5.77–5.79 (2H, m, OCH_2O); 6.16 (1H, s, H-1); 6.41–6.44 (1H, d, J = 8.58, H-11); 6.47–6.50 (1H, d, J = 8.01, Ar); 6.58 (1H, s, H-4); 6.60–6.63 (1H, d, J = 8.24, Ar); 6.68–6.72 (1H, d, J = 8.66, H-12); 7.18–7.26 (3H, m, Ar, H-4′); 8.43–8.46 (1H, d, J = 7.88, H-5′). ^{13}C NMR spectrum ($CDCl_3$), δ: 30.71; 42.89; 49.29; 56.27; 60.90; 101.18; 103.80; 107.91; 108.68; 111.87; 115.79; 117.03; 117.78; 118.20; 124.80; 125.00; 127.25; 128.54; 128.95; 130.48; 131.29; 131.82; 132.58; 132.75; 134.51; 139.81; 143.38; 143.47; 145.44; 148.01; 150.55; 150.73; 151.45; 200.30. Found, *m/z*: 656.1518 $[M+Na]^+$. $C_{34}H_{25}N_4NaO_9^+$. Calculated, *m/z*: 656.1519.

2-(9,10-Dimethoxy-13-(7-nitrobenzo[*c*][1,2,5]oxadiazol-4-yl)-5,8-dihydro-6*H*-[1,3]dioxolo[4,5-*g*]isoquinolino[3,2-*a*]isoquinolin-8-yl)-1-(3,4-dimethoxyphenyl)ethan-1-one (6).

Yield 487 mg (72%), dark-green needle-shaped crystals, decomp. 143–144°C. ^{1}H NMR spectrum (DMSO-d_6), δ (J, Hz): 2.76 (2H, br.s., 5-CH_2); 3.00–3.07 (1H, m, 5-CH_2); 3.44–3.57 (2H, m, 6-CH_2, $CH_2C(O)$); 3.66 (3H, s, 3-OCH_3); 3.74 (3H, s, 4-OCH_3); 3.76 (3H, s, 10-OCH_3); 3.78–3.81 (1H, m, $CH_2C(O)$); 3.83 (3H, s, 9-OCH_3); 5.48–5.53 (1H, d, J = 11.27, H-8); 5.80–5.83 (2H, d, J = 7.69, OCH_2O); 6.17 (1H, s, H-1); 6.56–6.60 (1H, d, J = 8.57, H-11); 6.79 (1H, s, Ar); 6.80–6.85 (2H, dd, J = 8.69, 3.64, Ar); 7.26 (1H, s, H-4); 7.34–7.37 (1H, d, J = 8.03, H-5′); 7.43–7.48 (1H, d, J = 8.46, H-12); 8.51–8.54 (1H, d, J = 8.06, H4′). ^{13}C NMR spectrum (DMSO-d_6), δ: 25.94; 26.80; 29.85; 49.30; 56.68; 60.91; 65.39; 101.71; 105.12; 108.34; 108.67; 110.62; 111.13; 112.67; 119.16; 123.63; 124.69; 125.26; 127.46; 130.01; 133.02; 133.10; 137.85; 137.91; 143.27; 144.28; 145.54; 148.35; 148.92; 150.80; 151.33; 153.62; 196.51. Found, *m/z*: 701.1861 $[M+Na]^+$. $C_{36}H_{30}N_4NaO_{10}^+$. Calculated, *m/z*: 701.1860.

2-Chloro-2-(9,10-dimethoxy-13-(7-nitrobenzo[*c*][1,2,5]oxadiazol-4-yl)-5,8-dihydro-6*H*-[1,3]dioxolo[4,5-*g*]isoquinolino[3,2-*a*]isoquinolin-8-yl)acetonitrile (7).

Yield 240 mg (42%), dark-green needle-shaped crystals, decomp. 103–105°C. ^{1}H NMR spectrum ($CDCl_3$), δ (J, Hz): 2.97–3.11 (2H, m, 5-CH_2); 3.54–3.65 (2H, m, 6-CH_2); 3.83 (3H, s, 10-OCH_3); 3.86 (3H, s, 9-OCH_3); 4.90–4.92 (1H, d, J = 5.71, CHCl); 5.10–5.12 (1H, d, J = 5.76, H-8); 5.98 (2H, s, OCH_2O); 6.13 (1H, s, H-1); 6.75–6.81 (2H, m, H-4, H-11); 6.97–7.00 (1H, d, J = 8.44, H-12); 7.96–7.99 (1H, d, J = 7.91, H-4′); 8.62–8.65 (1H, d, J = 7.89, H-4′). ^{13}C NMR spectrum (DMSO-d_6), δ: 30.22; 44.64; 49.22; 56.57; 61.09; 95.95; 101.53; 104.51; 108.58; 114.68; 116.78; 117.62; 118.26; 119.10; 124.88; 128.09; 128.49; 129.19; 132.41; 132.97; 134.72; 137.21; 143.86; 145.04; 145.43; 149.83; 150.66. Found, *m/z*: 595.0870 $[M+Na]^+$. $C_{28}H_{19}ClN_5NaO_7^+$. Calculated, *m/z*: 595.0871.

Gravimetric, polarization and impedance measurements were carried out on low-carbon steel in 1 M hydrochloric acid solution without and with the additives at

concentrations of 10^{-5}–10^{-4} mol/L. The measurement technique is described in detail elsewhere [10].

Results and Discussion

The degree of protection of the studied compounds is presented as a function of their concentration in Figure 1.

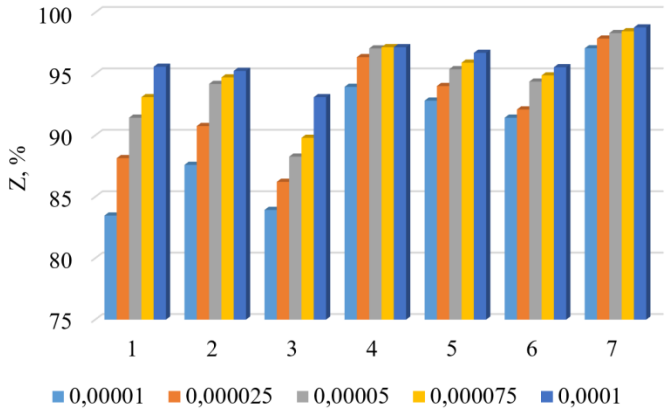

Figure 1. Dependence of the degree of protection on the nature of the substituent and the concentration of the additive *C*, mol/L.

All the additives synthesized act as corrosion inhibitors of steel; the protective effect increases with increasing concentration. Compounds **4**, **5**, **6**, and **7** are most efficient: their protective effects exceed 91% even at the lowest concentration. The efficiency of compounds **1**, **2**, and **3** depends on the concentration to a greater extent: *Z* exceeds 91% only at *C* greater than 0.05 mmol/L (**1**, **2**) or *C* = 0.1 mmol/L (**3**).

Based on the available data, the effect of the structure of compounds on their efficiency can be analyzed qualitatively. As it can be seen, the studied compounds either differ in the nature of the substituent and its position in the phenyl radical (**1**, **2**, **3**, **5**, and **6**), or the ring contains a heteroatom –N(4), or a –CHClCN group. This enables comparison of the effect of various substituents located at the same position (**1** and **3**, **2** and **5**), the effect of the position of the same substituent (**1** and **2**), and the effect of the same element (nitrogen) located in the functional group or in a ring (**3** and **4**). At most concentrations, the meta position in the phenyl radical is more preferable for bromine (compounds **1** and **2**), Figure 1. The protective effect of a compound with bromine at the *ortho* position (**1**) is higher than when this position is occupied by an amino group (**3**). A compound containing a hydroxy group at a *meta* position (**5**) is also more efficient than a compound with bromine at the same position (**2**). Compounds **4** and **7** are characterized by the best protective properties. Moreover, the presence of nitrogen in the heterocycle (**4**) turned out to be more preferable compared to its presence in a functional group (**3**). Due to the presence of a nitrile group in compound **7**, it can acquire film-forming properties.

The calculated parameters of the studied compounds are presented in Table 1.

Table 1. Calculated parameters of molecules.

Parameter	Value of the parameter for compounds						
	1	**2**	**3**	**4**	**5**	**6**	**7**
E_{HOMO}, **eV**	–4.714	–4.728	–4.725	–4.73	–4.65	–4.62	–4.936
E_{LUMO}, **eV**	–3.394	–3.39	–3.423	–3.395	–3.33	–3.294	–3.697
μ, D	7.826	9.86	8.095	10.339	8.937	10.349	7.813
ΣED	0.155	0.066	–0.368	0.349	–0.059	–0.198	0.623
Δ*E*, eV	–1.32	–1.338	–1.302	–1.335	–1.32	–1.326	–1.239
χ	4.054	4.059	4.074	4.063	3.99	3.957	4.317
η	0.661	0.669	0.651	0.668	0.662	0.663	0.619
σ	1.515	1.495	1.536	1.498	1.515	1.508	1.614

Let us consider the correlation between the efficiency and calculated parameters of the molecules. Figure 2 shows the correlation coefficients of the γ–*X* linear plots, where *X* is a calculated parameter from Table 1.

At a temperature of 298 K, a strong correlation (78–83%) is observed between the efficiency of the additives and the calculated parameters of the molecules, with the exception of the dipole moment (Figure 2a). As the temperature increases, the correlation deteriorates in most cases (Figure 2b). However, it should be noted that the correlation coefficients of the linear plots, even at a temperature of 298 K, are inferior to the *R* values obtained in [10].

The dependence of the logarithm of the inhibition coefficient on the logarithm of concentration is linear in most cases (Figure 3).

Hence, surface blocking contributes to the reduction of the corrosion rate of steel in the presence of the compounds studied.

The data obtained from gravimetric measurements are linearized in the Langmuir isotherm coordinate system with correlation coefficients of 98.88–99.98%. This circumstance made it possible to calculate the free energy of adsorption of compounds using Equation 1, Table 2.

$$\Delta G_{ads} = -RT \ln(5.55B) \quad (1)$$

where *B* is the adsorption constant.

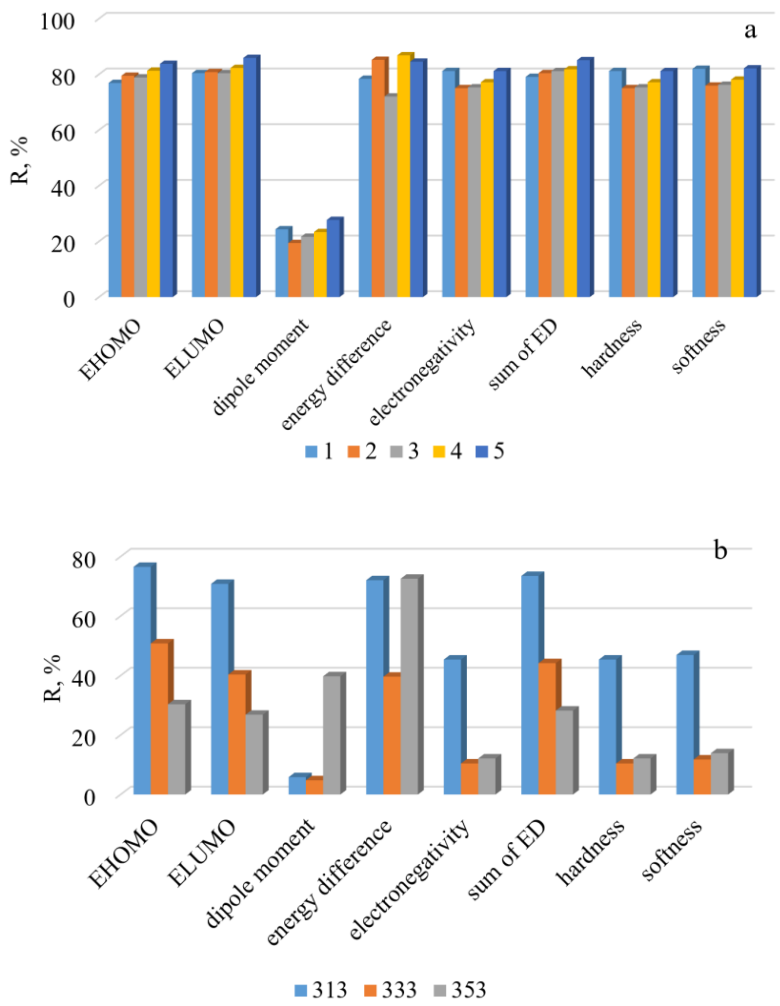

Figure 2. Correlation coefficients for the γ-X plots at a temperature of 298 K as a function of the concentration of compounds (a): 0.01 (**1**), 0.025 (**2**), 0.05 (**3**), 0.075 (**4**), 0.1 (**5**) mmol/L and (b): at temperatures *T*, K at *C* = 0.1 mmol/L.

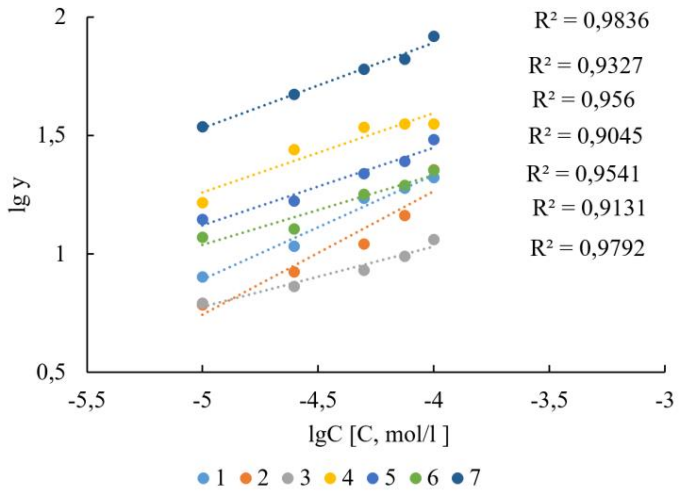

Figure 3. Dependence of the inhibition coefficient on the concentration of the additives.

Table 2. Dependence of some parameters on the nature of the additive.

Parameter	Value of the parameter for additives						
	1	**2**	**3**	**4**	**5**	**6**	**7**
E_{ac}, **kJ/mol**	72.4	71.2	93.4	83.4	79.1	86.2	65.3
$-\Delta G_{ads}$, **kJ/mol**	38.9	39.2	39.3	38.9	35.6	34.9	41.3
***Z*, %**	95.6	95.3	93.1	97.2	96.7	95.6	98.8
θ, %	90.9	85.5	90.1	82.9	86.8	66.5	84.9

Note: E_{ac}, Z, and θ are determined at C = 0.1 mmol/L; E_{ac} in 1 M HCl solution is 72 kJ/mol.

Compound **7** is characterized by only chemical adsorption (ΔG_{ads} <–40 kJ/mol); in the case of the other compounds, both physical and chemical adsorption occur (–20 kJ/mol< ΔG_{ads} <–40 kJ/mol). The low ΔG value of compound **7** can be attributed to the presence of a triple bond in the nitrile group.

It should be noted that with increasing temperature, all compounds retain a high protective effect against steel corrosion; the efficiency of inhibitors is above 90%, except for additive **3** at T = 353 K.

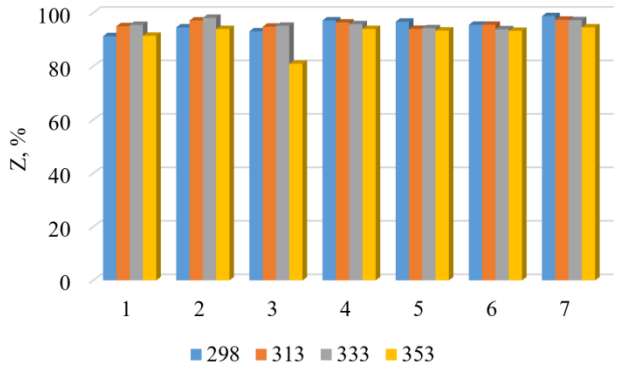

Figure 4. Dependence of the degree of protection on the nature of the additive and temperature T, K at C = 0.1 mmol/L.

The effective activation energies of steel corrosion in the presence of the additives in the acid are presented in Table 1. The compounds studied either do not affect (**1**, **2**), or increase (**3**–**6**), or slightly reduce the effective activation energy of the corrosion process. The first and last effects can be due to surface blocking, a change in the process mechanism, or an increase in the degree of surface coverage with increasing temperature.

The Nyquist plots obtained for steel in solutions of hydrochloric acid without and with the additives at all concentrations studied have a qualitatively similar appearance (Figure 5).

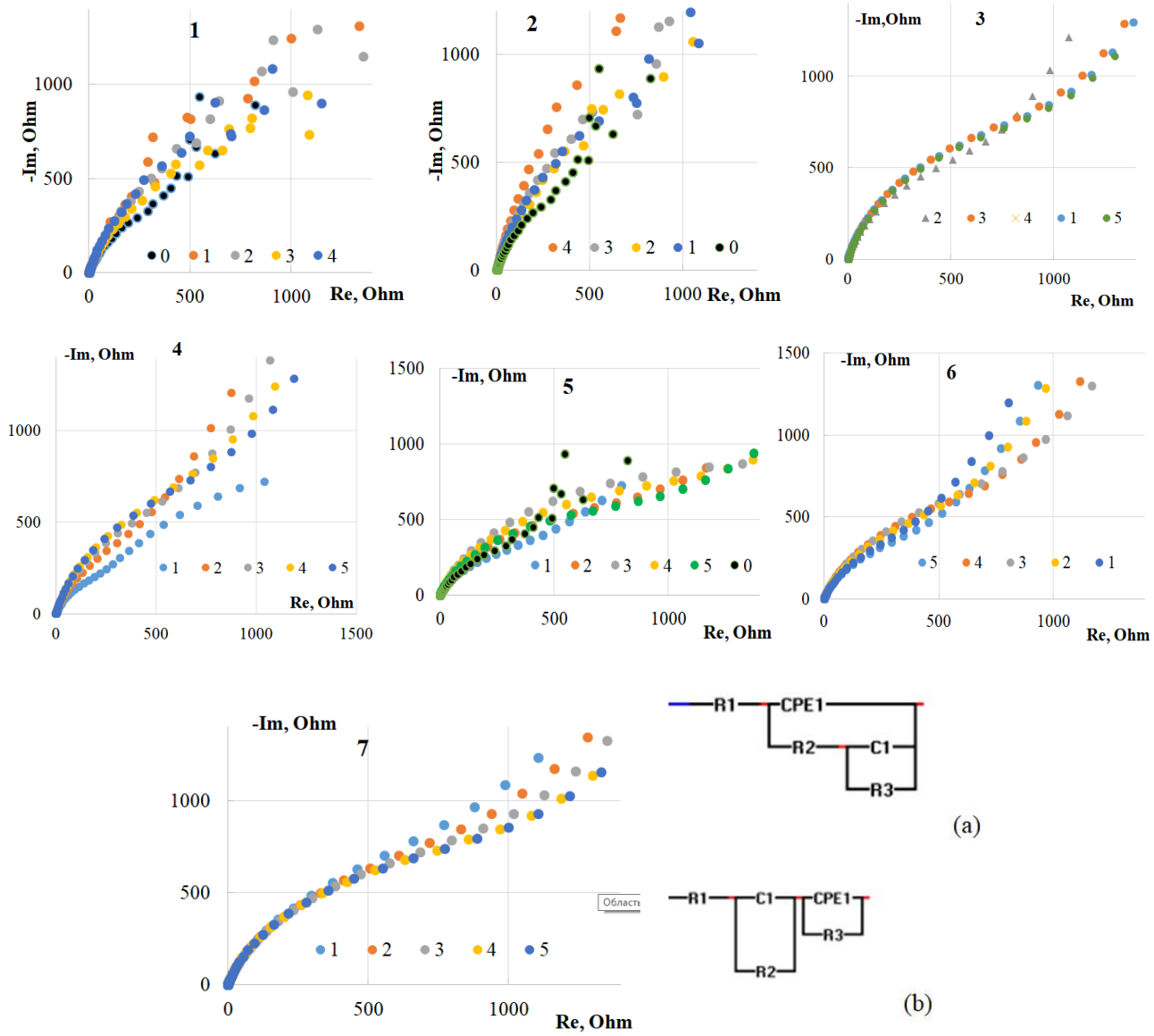

Figure 5. Nyquist plots of steel in 1 M hydrochloric acid without an inhibitor (0) and in the presence of the inhibitors at *C*, mmol/L: 0.01 (1), 0.025 (2), 0.05 (3), 0.075 (4), and 0.1 (5). The digits on the plots indicate numbers of the additives.

In most cases, the minimum disagreement between the obtained and calculated impedance data was observed when using equivalent circuits (a) and (b), Figure 5. The double electric layer capacitance was used to calculate the degree of surface coverage with inhibitors (θ), Table 2. For all the compounds, $\theta < Z$ (Table 2), which indicates a mixed mechanism of their action.

The polarization curves obtained on steel in the hydrochloric acid solution without (0) and in the presence of inhibitors have a qualitatively similar appearance. Some of them are shown in Figure 6.

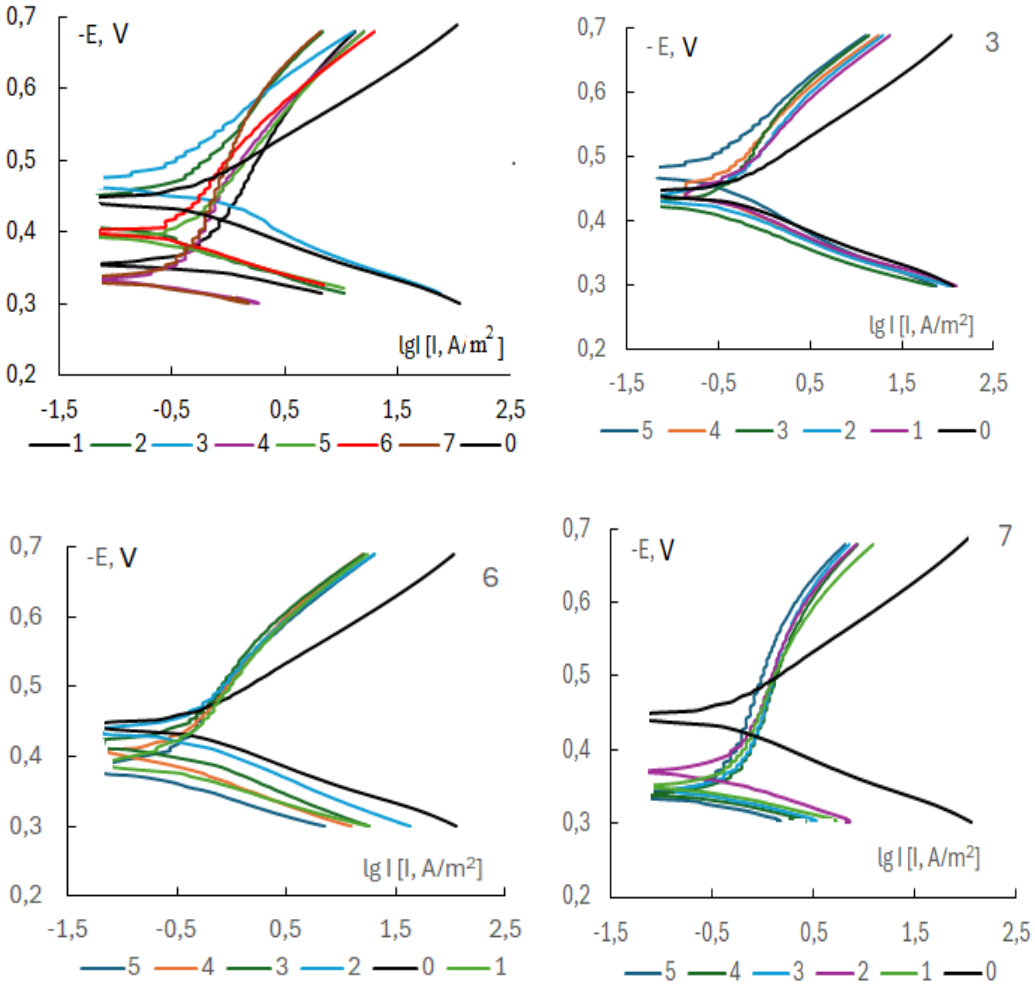

Figure 6. Polarization curves of steel in hydrochloric acid solution without (0) and in the presence of inhibitors (**1**–**7**) at *C* = 0.1 mmol/L and in the presence of compounds **3**, **6**, and **7** at *C*, mmol/L: 0.01 (**1**), 0.025 (**2**), 0.05 (**3**), 0.075 (**4**), 0.1 (**5**).

All the compounds are mixed type inhibitors with a predominant effect on the anodic reaction. They increase the corrosion potential and the polarizability of the cathodic reaction. Compound **3** at the highest concentration predominantly inhibits the cathodic reaction and reduces the corrosion potential, Figure 6.

Conclusions

1. The new isoquinoline derivatives are mixed inhibitors of steel corrosion in hydrochloric acid.
2. The compounds are adsorbed on the surface of steel due to physical and chemical forces. Their adsorption is described by the Langmuir isotherm.
3. The inhibitors have an activation–blocking mechanism of the protective action.
4. The efficiency of the additives satisfactorily correlates with the calculated parameters of the molecules.

References

1. Ya.G. Avdeev and M.V. Tyurina, Inhibition of acid corrosion of metals by N-containing six-membered heterocycles: a review, *Korroz.: Mater., Zashch. (Corrosion: materials, protection)*, 2017, **5**, 1–15 (in Russian)
2. Ya.G. Avdeev, K.L. Anfilov and Yu.I. Kuznetsov, Effect of nitrogen-containing inhibitors on the corrosion inhibition of low-carbon steel in solutions of mineral acids with various anionic compositions, *Int. J. Corros. Scale Inhib.*, 2021, **10**, 1566–1586. doi: 10.17675/2305-6894-2021-10-4-12
3. A.G. Berezhnaya, V.V. Chernyavina and I.I. Krotkii, Derivatives of pyrilium perchlorate and berberine as inhibitors of steel corrosion in hydrochloric acid, *Korroz.: Mater., Zashch. (Corrosion: materials, protection)*, 2022, **2**, 37–42 (in Russian). doi: 10.31044/1813-7016-2022-0-2-37-42
4. A. Mohammed, H.S. Aljibori, M.A.I. Al-Hamid, W.K. Al-Azzawi, A.A.H. Kadhum and A. Alamiery, N-Phenyl-N′-[5-phenyl-1,2,4-thiadiazol-3-yl]thiourea: corrosion inhibition of mild steel in 1 M *HCl*, *Int. J. Corros. Scale Inhib.*, 2024, **13**, 38–78. doi: 10.17675/2305-6894-2024-13-1-3
5. J.A. Ibrahim, H.H. Ibraheem and H.T. Hussein, Experimental and theoretical studies on the corrosion inhibition potentials of N′-((1H-indole-3-yl)methylene)benzohydrazide for mild steel in HCl, *Int. J. Corros. Scale Inhib.*, 2024, **13**, 94–120. doi: 10.17675/2305-6894-2024-13-1-6
6. M.D. Plotnikova, A.B. Shein, M.G. Scherban, A.N. Vasyanin and A.E. Rubtsov, Experimental and theoretical investigation of (E)-5-{[4-(dimethylamino)benzylidene] amino}-1,3,4-thiadiazole-2(3H)-thione (DATT) as an acid corrosion inhibitor of mild steel, *Int. J. Corros. Scale Inhib.*, 2023, **12**, 1365–1391. doi: 10.17675/2305-6894-2023-12-4-1
7. M. Bouziani Idrissi, H. Hailou, I. Filali, M. Rbaa, F. Benhiba, K. Nouneh, E. El Kafsaou, C. El Mahjoub, A. El Midaoui, H. Oudda and A. Zarrouk, Theory and experimental investigations on the effect of the halogenated chain of new synthesis compounds based on benzimidazole derivatives on the inhibition corrosion of mild steel in acid media, *Int. J. Corros. Scale Inhib.*, 2023, **12**, 1535–1563. doi: 10.17675/2305-6894-2023-12-4-8
8. D.V. Lyapun, D.S. Shevtsov, A.A. Kruzhilin, O.A. Kozaderov, I.V. Avetisyan, D.A. Machnev, I.D. Zartsyn and Kh.S. Shikhaliev, Inhibition of low-carbon steel corrosion by derivatives of 4,5,6,7-tetrahydro-[1,2,4]triazolo[1,5-a]pyrimidin-7-ol, *Int. J. Corros. Scale Inhib.*, 2023, **12**, 2256–2264. doi: 10.17675/2305-6894-2023-12-4-43
9. A. Elbarki, Z. Amrani, T. Laabaissi, M. El Faydy, L. Adlani, A. Fatah, F. Benhiba, M. Rbaa, Warad, B. Lakhrissi, H. Zarrok, A. Bellaouchou, B. Dikici, H. Oudda and A. Zarrouk, The inhibitory effect of certain imidazole derivatives grafted on 8-hydroxyqinoline on carbon steel corrosion in acidic medium: experimental and

computational approaches, *Int. J. Corros. Scale Inhib*., 2023, **12**, 1292–1320. doi: 10.17675/2305-6894-2023-12-3-27

10. A.G. Berezhnaya, A.D. Zagrebaev, V.V. Chernyavina and I.I. Krotkii, Chernyavskaya V.V. Novel isoquinolinium derivatives as inhibitors of acid corrosion, *Int. J. Corros. Scale Inhib*., 2024, **13**, 311–323. doi: 10.17675/2305-6894-2024-13-1-15
11. V.P Grigor'ev and V.V. Ekilik, *Chemical structure and protective action of corrosion inhibitors*, Rostov, University, 1978, 184 pp. (in Russian).
12. A.D. Zagrebaev, O.N. Burov, M.E. Kletskii, A.V. Lisovin, S.V. Kurbatov and O.D. Demekhin, The Synthesis and Investigation of New Electroneutral Berberine Derivatives, *Chem. Heterocycl. Compd*., 2022, **58**, 45–57. doi: 10.1007/s10593-022-03055-0
13. O.D. Demekhin, O.N. Burov, M.E. Kletskii, S.V. Kurbatov, E.A. Bereznyak, and A.V. Trishina, A Structural Modification of Berberine Using CH Acids and Ethoxyethylenes Based on Them, *Chem. Heterocycl. Compd*., 2022, **58**, 621–627. doi: 10.1007/s10593-022-03135-1
14. O.N. Burov, S.V. Kurbatov, M.E. Kletskii, A.D. Zagrebaev and I.E. Mikhailov, Synthesis and structure of dihydroberberine nitroaryl derivatives – potential ligands for G-quadruplexes, *Chem. Heterocycl. Compd*., 2017, **53**, 335–340. doi: 10.1007/s10593-017-2055-3
15. O.N. Burov, S.V. Kurbatov, P.G. Morozov, M.E. Kletskii and A.V. Tatarov, Synthesis of the first 13-nitroaryl derivatives of 8-acetonylberberine, *Chem. Heterocycl. Compd*., 2015, **51**, 772–774. doi: 10.1007/s10593-015-1774-6
16. A.D. Zagrebaev, V.V. Butova, A.A. Guda, S.V. Chapek, O.N. Burov, S.V. Kurbatov, E.Yu. Vinyukova, M.E. Neganova, Yu.R. Aleksandrova, N. Nikolaeva, O.P. Demidov and A.V. Soldatov, Optimal synthesis conditions for NBF-modified 8, 13-dihydroberberine derivatives, *New J. Chem*., 2024, **48**, 268–280. doi: 10.1039/D3NJ04562E

♦ ♦ ♦